Intercage Electron Transfer Driven by Electric Field in Robin-Day-Type Molecules

ARTICLE *in* CHEMPHYSCHEM · FEBRUARY 2012

Impact Factor: 3.42 · DOI: 10.1002/cphc.201100790 · Source: PubMed

7 AUTHORS, INCLUDING:

Yin-Feng Wang
Jinggangshan University
20 PUBLICATIONS **177** CITATIONS
SEE PROFILE

Zhong-Jun Zhou
Jilin University
28 PUBLICATIONS **241** CITATIONS
SEE PROFILE

Di Wu
Nanjing University
440 PUBLICATIONS **6,033** CITATIONS
SEE PROFILE

feng long gu
South China Normal University
104 PUBLICATIONS **1,747** CITATIONS
SEE PROFILE

CHEMPHYSCHEM

DOI: 10.1002/cphc.201100790

Intercage Electron Transfer Driven by Electric Field in Robin–Day-Type Molecules

Yin-Feng Wang,[a, b] Ying Li,[a] Zhong-Jun Zhou,[a] Zhi-Ru Li,*[a] Di Wu,[a] Jiangen Huang,[b] and Feng Long Gu*[c]

A new class of isomers, namely, intercage electron-transfer isomers, is reported for fluorinated double-cage molecular anion $e^-@C_{20}F_{18}(NH)_2C_{20}F_{18}$ with $C_{20}F_{18}$ cages: **1** with the excess electron inside the left cage, **2** with the excess electron inside both cages, and **3** with the excess electron inside the right cage. Interestingly, the $C_{20}F_{18}$ cages may be considered as two redox sites existing in a rare nonmetal mixed-valent (0 and −1) molecular anion. The three isomers with two redox sites may be the founding members of a new class of mixed-valent compounds, namely, nonmetal Robin–Day Class II with localized redox centers for **1** and **3**, and Class III with delocalized redox centers for **2**. Two intercage electron-transfers pathways involving transfer of one or half an excess electron from one cage to the other are found: 1) Manipulating the external electric field (−0.001 a.u. for **1**→**3** and −0.0005 a.u. for **1**→**2**) and 2) Exciting the transition from ground to first excited state and subsequent radiationless transition from the excited state to another ground state for **1** and **3**. For the exhibited microscopic electron-transfer process **1**→**3**, **2** may be the transition state, and the electron-transfer barrier of 6.021 kcal mol^{-1} is close to the electric field work of 8.04 kcal mol^{-1}.

1. Introduction

Isomerism is a central concept in chemistry that is constantly being enriched.[1,2] Isomerism due to electron transfer is very interesting due to special properties and applications of such systems in molecular electronics. Mixed-valent complexes with intervalence charge transfer (IVCT) properties have become the focus of recent research for a number of reasons. These include their role in biochemistry, their model character for intramolecular electron transfer, their unusual spectroscopic properties, their potential in molecular electronics, and their function as test systems for theoretical approaches.[3–5]

Forty years ago, Robin and Day introduced the systematic basis upon which all mixed-valent complexes are classified.[6] In the first designed mixed-valent complexes, which were prepared by Creutz and Taube,[7] the mixed-valent ion is known as the Creutz–Taube ion. In recent years, there has been particular interest in the sometimes vague boundary between weakly localized (Class II) and fully delocalized (Class III) systems. Meyer et al. discussed the localized-to-delocalized transition in mixed-valent chemistry, and proposed the defining characteristics of a new class of mixed-valent complexes, namely, Class II–III.[8] For intervalence charge-transfer systems, novel donor–acceptor systems have been reported, particularly those based on purely organic species and those at the borderline between Classes II and III.[9,10]

The excess electron can be trapped inside a cavity (cage) formed by some surrounding polar solvent molecules in liquid and molecular clusters to form solvated electrons. The investigation of the solvated electron plays a prominent role in physics, chemistry, and biochemistry.[11,12] Stabilization and manipulation of a bound electron are important in molecular clusters and nanodevices[13] and could provide new approaches to preparing conductive and unusual optical[14] or magnetic materials.[15] In previous studies, stabilization of an excess electron was realized inside single-molecular perfluorinated carbon cages[16–18] including $C_{20}F_{20}$.[19] The resulting single-molecular solvated electron system is more stable than the molecular cluster solvated electron[20] due to the covalent cage acting as a special electron hole.[16]

An excess electron can be trapped inside single-molecular double cage $C_{20}F_{18}(NH)_2C_{20}F_{18}$ to form $e^-@C_{20}F_{18}(NH)_2C_{20}F_{18}$, which exhibits intercage electron-transfer transition involving the ground and first excited state potential surfaces.[18] The question therefore arises whether or not the excess electron has different distributions inside the double cage on the ground-state potential surface. This would result in an interesting and novel intercage electron-transfer isomerism phenom-

[a] Dr. Y.-F. Wang, Assist. Prof. Y. Li, Dr. Z.-J. Zhou, Prof. Z.-R. Li, Prof. D. Wu
State Key Laboratory of Theoretical and Computational Chemistry
Institute of Theoretical Chemistry
Jilin University
Changchun 130023 (China)
E-mail: lzr@jlu.edu.cn

[b] Dr. Y.-F. Wang, Prof. J. Huang
Jiangxi Province Key Laboratory of Coordination Chemistry
Institute of Applied Chemistry
Jinggangshan University
Ji'an, Jiangxi 343009 (China)

[c] Prof. F. L. Gu
Center for Computational Quantum Chemistry
South China Normal University, Guangzhou, 510631 (China)
E-mail: gu@scnu.edu.cn

Supporting information for this article is available on the WWW under http://dx.doi.org/10.1002/cphc.201100790.

enon in the nonmetal double-cage mixed-valent molecular anion.

Herein we report on our search for intercage electron-transfer isomers that show unusual chemical and physical properties and exhibit intercage electron-transfer isomerization pathways, revealing the nature of the electron in the electron-transfer process and enhancing knowledge on isomerism. This work may provide new approaches to designing unusual conductive, optical, and magnetic materials and molecular electronic devices.

Computational Details

We used the diffuse basis set 4s4p describing the excess electron[16,18,24] to optimize isomer structures of $e^-@C_{20}F_{18}(NH)_2C_{20}F_{18}$. The diffuse basis set 4s4p is put at the center of the left (or right) cage for the molecule to give the optimized structure of isomer **1** (or **3**). When the diffuse basis set is placed at the geometrical center of the molecule, the optimized isomer structure of **2** is obtained (the excess electron is divided into two half-electrons inside the two cages). Three different SOMOs can be obtained for the three optimized structures of **1**, **2**, and **3**.

For $e^-@C_{20}F_{18}(NH)_2C_{20}F_{18}$, optimized structures of the intercage electron-transfer isomers with all real frequencies were obtained at the B3LYP/6-31G(d)+4s4p level.[18] To check the credibility of symmetric isomer **2** (see Figure 1), the symmetric structure **2** with all real frequencies for $<s^2>=0.75$ was also obtained at the HF/6-31G(d)+4s4p level (without the self-interaction error), which shows that **2** is believable and does not come from the self-interaction error[29] of DFT for anions.

There is much literature on the controversy whether or not DFT can yield reasonably good adiabatic electron affinities (EAs) or vertical detachment energies (VDEs).[16,21,22] Schaefer and co-workers[21] demonstrated that DFT is indeed applicable to anions and provides EA predictions of open-shell systems. The EA and VDE of some cagelike single-molecular solvated-electron systems have been obtained with the B3LYP method.[16–18] For our large double-cage solvated electron systems, the long-range corrected functional should be considered. To find a suitable calculation method, we selected the relatively small solvated electron model system $e^-_2@(LiF)_6$[23] and calculated its VDE I & II with different methods (see Table S1 in the Supporting Information), as the VDE I and II of a dianion are related to the EA and VDE of the anion, respectively. Table S1 of the Supporting Information shows that the VDEs in the framework of long-range corrected Becke–Lee–Yang–Parr DFT (LC-BLYP) are close to those at the MP2 level.[23] In our previous study, the LC-BLYP/6-311++G(d,p)+6s6p4d level was selected to calculate the VDEs and vertical electron affinities (VEAs) of isomer **1** of $e^-@C_{20}F_{18}(NH)_2C_{20}F_{18}$.[19] Therefore, on the basis of the optimized neutral geometries of **1**, **2**, and **3**, the VDEs and VEAs of our open-shell structures were calculated at the LC-BLYP/6-311++G(d,p)+*6s6p4d* level according to Equations (1) and (2):

$$\mathrm{VDE} = E[\mathrm{M}] - E[\mathrm{M}^-] \quad (1)$$

$$\mathrm{VEA} = E[\mathrm{M}^-] - E[\mathrm{M}^{2-}] \quad (2)$$

In our previous study, when another excess electron was added to **1**, the resulting triplet dianions were more stable than the corresponding singlet dianions.[18] Therefore, we only consider the triplet dianions in the calculations of the VEAs.

The diffuse basis sets 4s4p and 6s6p4d were used to describe the characteristic of the excess electron.[16,18,24] Construction and locations of these diffuse basis sets are given in the Supporting Information (see Table S2). The spin contamination is negligible.

All calculations were carried out with the Gaussian 09 (Revision A.02) program package.[25]

2. Results and Discussion

2.1. Intercage Electron-Transfer Isomers

Optimized geometric structures and important parameters for isomers **1**, **2**, and **3** of the double-cage single-molecular solvated-electron system $e^-@C_{20}F_{18}(NH)_2C_{20}F_{18}$ are listed in Table 1. For each isomer of $e^-@C_{20}F_{18}(NH)_2C_{20}F_{18}$, the SOMO and the spin density distribution were calculated and are depicted in Figure 1.

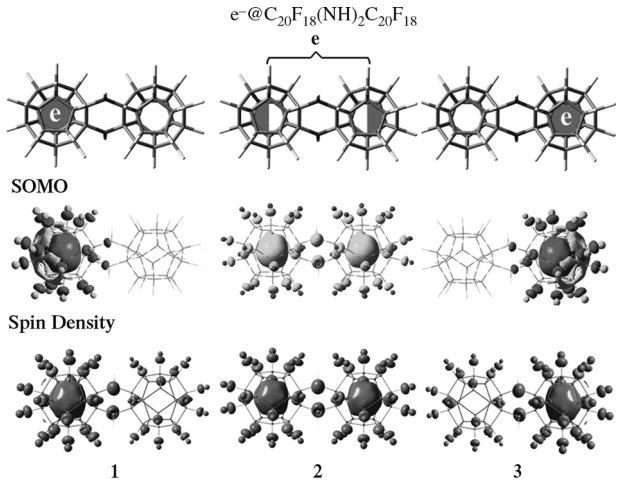

Figure 1. Structures, SOMOs (at an isovalue of 0.035 au), and spin densities (at an isovalue of 0.001 a.u.) of intercage electron-transfer isomers of $e^-@C_{20}F_{18}(NH)_2C_{20}F_{18}$.

Table 1. Structural parameters [Å] at the B3LYP/6-31G(d)+4s4p level.

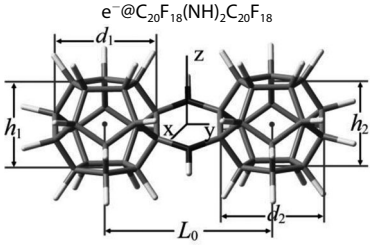

	1	2	3
Point group	C_2	C_{2h}	C_2
L_0	6.787	6.785	6.787
h_1	3.447	3.454	3.459
h_2	3.459	3.454	3.447
d_1	4.411	4.417	4.428
d_2	4.428	4.417	4.411

Table 1 shows small differences in molecular structures (δd, δh, or $\delta L_0 < 0.02$ Å) and Figure 1 shows different electronic structures for the three isomers **1**, **2** and **3**, which indicates that they are intercage electron-transfer isomers. Their s-type electron clouds indicate that, for isomers **1** and **3**, the excess electron is confined in the left and right $C_{20}F_{18}$ cage, respectively, while the excess electron is equally confined in both cages for **2**. As the self-interaction error in DFT may lead to artificial stabilization of delocalized states, most evident in systems with an odd number of electrons,[26–28] the credibility of isomer **2** should be checked by Hartree–Fock (HF) calculation without the self-interaction error.[29] The symmetric structure **2** with all real frequencies for $<s^2> = 0.75$ was obtained at the HF/6-31G(d) + 4s4p level, which shows that **2** with the excess electron equally confined in both cages is believable.

For the hydrated electron in water under normal and supercritical conditions, molecular dynamics simulations were performed.[30a] The s-type electron clouds of these intercage electron-transfer isomers are obviously differently from that reported for the hydrated electron, in which the spatial distribution of the electronic cloud of the e^-_{aq} often departs from an isotropic s-like shape.[30a] For the endohedral metallofullerene $Sc@C_{82}$, most of the electron spin density is distributed around the carbon cage, but 5% of it is inside the carbon cage,[30b] in contrast to intercage electron-transfer isomers with the distribution of electron spin density inside the cage.

Interestingly, the two $C_{20}F_{18}$ cages can trap an excess electron inside them, so they may be considered as two redox sites existing in the rare nonmetal mixed-valent (0 and −1) molecular anion. The three isomers of the two redox sites may be the founding members of a new class of mixed valence molecules, namely, nonmetal Robin–Day Classes II and III. Compounds **1** and **3** with localized redox centers may be the founding members of Class II, and **2** with delocalized redox centers the founding member of Class III. Owing to different electron-transfer states, **1**–**3** are a new kind of isomers and are denoted intercage electron-transfer isomers: **1** with an excess electron trapped inside the left cage (−1 and 0 valences), **2** with the electron equally confined inside the two cages (0.5 and 0.5 valences), and **3** with the electron inside the right cage (0 and −1 valences).

Considering the interaction between the excess electron and the cages, we compare the sizes (h and d) of cages for the intercage electron-transfer isomers. From Table 1, the order of the sizes of the fluorinated cages is cage with an excess electron (left h_1 and d_1 for **1** and right h_2 and d_2 for **3**) < cage with half an electron in **2** ($h_1 = h_2$ and $d_1 = d_2$) < cage without excess electron (right h_2 and d_2 for **1** and left h_1 and d_1 for **3**). This result indicates that the size of the fluorinated cage slightly decreases (< 0.01 Å for h and d) with increasing electron occupation number (0, 0.5, and 1). The existence of the excess electron makes the occupied cage shrink slightly, which is the geometrical effect of the excess electron on the cage. The shrinkage of the cage slightly increases the electronic attraction due to the enhanced interior attractive potential, which is beneficial for localization of an excess electron.

2.2. Physical and Chemical Properties

Comparing the total energies of **1**, **2**, and **3** at the LC-BLYP/6-311++G(d,p)+6s6p4d level (see Table 2), we find that the relative energies are 0.0 (**1**), 6.02 (**2**), and 0.0 kcal mol^{-1} (**3**). These small energy differences indicate small differences in thermodynamic stability.

Table 2. Total energies E_{tot} [a.u.], relative energies E_{rel} [kcal mol^{-1}], dipole moments μ_y [D], LUMO–HOMO gaps E_{gap} [eV], vertical detachment energies (VDE) [eV], and vertical electron affinities (EA) [eV] at the LC-BLYP/6-311++G(d,p)+6s6p4d level.

	$e^-@C_{20}F_{18}(NH)_2C_{20}F_{18}$		
	1	**2**	**3**
E_{tot}	−5220.8131	−5220.8035	−5220.8131
E_{rel}	0.0	6.021	0.0
μ_y	13.4	0.0	−13.4
LUMO	−0.847	−1.337	−0.847
HOMO	−4.305	−3.607	−4.305
E_{gap}	3.458	2.270	3.458
VDE	3.660	3.324	3.660
VEA(t)	1.418	1.695	1.418

For $e^-@C_{20}F_{18}(NH)_2C_{20}F_{18}$, the low VDE implies that the excess electron from the SOMO is easily extracted, that is, it is easily oxidized, while the large VEA implies that on adding another excess electron to the SOMO or LUMO more energy is released, so it is easily reduced. Therefore, the small VDE is related to the high reducibility and the large VEA to high oxidation activity. From Table 2, the VDEs are 3.660 (**1**), 3.324 (**2**), and 3.660 (**3**) eV at the LC-BLYP/6-311++G(d,p)+6s6p4d level, which are larger than the VDE of 3.3 eV for the stable hydrated electron[31a] and less than that of 3.893 eV for the Cs atom.[31b] Thus, their stabilities are higher than that of the hydrated electron, and their reducibilities are slightly higher than that of the Cs atom. For VEA calculations, the used triplet state is lower than the singlet state for corresponding dianions,[19] so the VEA is named VEA(t). The VEA(t) values of 1.418 (**1**), 1.695 (**2**), and 1.418 eV (**3**) are close to that of 1.47 eV for the O atom.[31b] Thus the intercage electron-transfer isomers exhibit strong oxidizabilities close to that of the O atom. In summary, these intercage electron-transfer isomers have special chemical activities, not only high reducibility but also strong oxidizability, as each has a loosely bound electron as well as the $C_{20}F_{18}$ electron-hole cage with large interior electronic attractive potential.

The order of relative energies is **1** = **3** < **2**. The order of VDEs is **1** = **3** > **2**. The orders of both relative energies and VDEs indicate that the excess electron slightly prefers to reside in one cage to form **1** or **3** rather than symmetrically distribute over both cages to form **2**. The different spatial localizations of the excess electron lead to clearly different dipole moments (Table 2). The μ_y values of 13.4 (**1**), 0.0 (**2**), and −13.4 D (**3**) show that spatial localization of electron is closely related to this physical property described by a tensor.

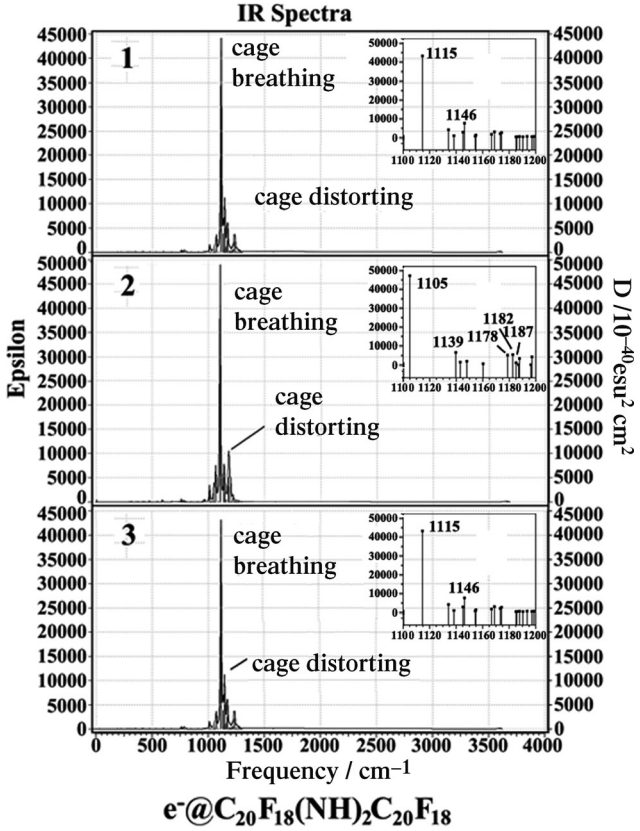

Figure 2. Calculated IR adsorption spectra of intercage electron-transfer isomers of $e^-@C_{20}F_{18}(NH)_2C_{20}F_{18}$.

To assist experimentalists in identifying the intercage electron-transfer isomers, the calculated IR adsorption spectra are depicted in Figure 2. The first and the second high peak correspond to a prominent breathing vibration mode and a minor distortion mode, respectively. The breathing vibration mode for the first peak is mainly expansion of one cage along with shrinking of the other. The $\tilde{\nu}$ value of 1115 cm^{-1} for the breathing vibration of **1** or **3** with two slightly different cages is slightly larger than that of 1105 cm^{-1} for **2** with two identical cages, while the peak intensity of the former is lower than that of the latter. For the second peak at $\tilde{\nu}=1146$ cm^{-1} in **1** and **3**, the minor distortion mode mainly involves expansion of one side along with shrinking of other side for one cage in the direction of the *y* axis. For **2**, the second peak is superimposed by three small minor distortion modes with approximately the same frequency ($\tilde{\nu}=1178$, 1182, and 1187 cm^{-1}). The small differences in structures are the origin of the small differences in the IR absorption spectra for the isomers.

2.3. Isomerization through Intercage Electron Transfer

For the intercage electron transfer isomers, their interconversion pathways are of special interest. We have used an external electric field to push a proton and performed proton transfer between HCl and NH_3.[32] The excess electron with charge can be easily driven by an electric field. Thus, we assumed that a physical method of manipulating the external electric field can realize interconversion among the current intercage electron-transfer isomers. Figure 3 shows that applying an external electric field of −0.0005 a.u. (−0.0257 V Å^{-1}) in the *y*-axis direction of **1** results in transfer of half an electron (see SOMO) from the left cage to the right cage, and then **1** with electron inside the left cage changes into **2** with the electron equally confined inside the two cages. Similarly, on applying an electric field of −0.0005 a.u. in the *y*-axis direction of **2**, the remaining half-electron (see SOMO) transfers from the left cage to the right cage, and then **2** transforms into **3** with the electron inside the right cage. Considering the electron transfer course (**1**→**2**→**3**), **2** may be the electron-transfer transition state between **1** and **3**. An electric field of −0.0010 a.u. can result in conversion from **1** to **3** by transferring an electron. By applying a suitable positive electric field of 0.0005 or 0.0010 a.u., the corresponding reverse reaction can also be performed. Therefore, interconversion among these intercage electron-transfer isomers can be realized by using a suitable external homogeneous electric field.

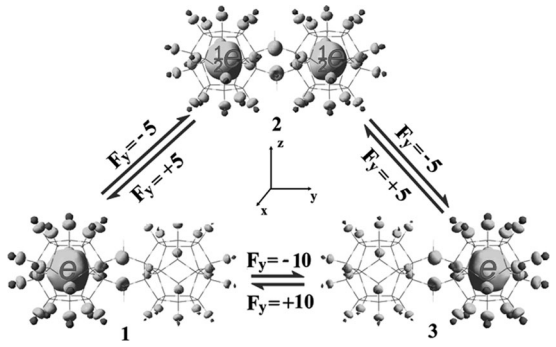

Figure 3. Conversion among the intercage electron-transfer isomers can be realized by manipulating the homogeneous electric field ($F_y=10^{-4}$ a.u.).

Previously, we reported on intercage excess electron transfer transition exhibited by **1**.[18] The transition with a transition energy of 1.70 eV from the ground state (excess electron inside left cage) to the first excited state (electron inside the right cage) causes the excess electron to transfer from the left cage to the right one.[18] Interestingly the first excited state of **1** with a transition energy of 1.70 eV is similar to the ground state of **3** without the transition energy due to keeping the electron inside the right cage. Then, the second pathway of isomerization between **1** and **3** can be found.

Figure 4 shows that a transition from the ground state of **1** to its first excited state and a subsequent radiationless transition from the excited state of **1** to the ground state of **3** may result in the conversion from **1** to **3**. Clearly, the mirror image relationship between **1** and **3** is exhibited for ground and the first excited states in Figure 4, so the two conversions from **1** to **3** and from **3** to **1** have a mirror-image relationship.

2.4. Transition State and Barrier for the Microscopic Electron-Transfer Process

It is well known that electron transfer reactions are important for chemical and biological phenomena.[33,34] Recently, research

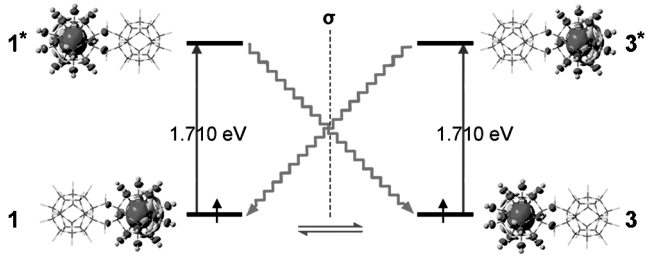

Figure 4. Mirror-image relationship for conversion between electron-transfer isomers **1** and **3** at the CIS/6-31G(d) level.

has mainly focused on phenomenological theory.[35–37] In researched electron-transfer processes, electron transfer takes place to cations and atoms with high electronegativity to form the reduced states. Electron transfer to form three-electron bonds is also reported.[37] The analysis of electron-transfer barriers is reported.[8] Here, electron transfers takes place as an intercage process for $e^-@C_{20}F_{18}(NH)_2C_{20}F_{18}$.

The energy levels of isomers **1** and **3** are degenerate. Conversion between **1** and **3** is a microscopic electron-transfer process without proton transfer. The cage $C_{20}F_{18}$ may be referred to as an electron hole cage due to the trapped electron. The electron-hole cage in a neutral molecule comes from double electric layers, which here are the positive inner spherical shell of C atoms and the negative outer shell of F atoms. It is different from an electron hole in crystals formed by taking away an anion.

Considering electron-transfer transition states is interesting and difficult.[38] From Table 2, the energy levels of **1** and **3** are degenerate, while **2** is only 6.021 kcal mol^{-1} higher than **1** and **3**. The small energy differences among them mainly come from the slight excess-electron effect on the cage geometry. The potential curve of the electron-transfer process between 1 and 3 is shown in Figure 5, which depicts the potential as a function of electronic coordinate. The horizontal axis represents the electron-transfer axis. We found that the electron-transfer transition state between **1** and **3** may be just **2**. The electron-transfer transition state has no imaginary frequency of atomic vibration. An imaginary atomic vibration frequency is necessary for conventional atom- or group-transfer reaction. For the electron-transfer transition state, an imaginary frequency of atomic vibration is not necessary, but an imaginary frequency of unknown excess electronic vibration may be necessary. In the electron-transfer process, half an electron transfers from the left cage to the right cage of **1**, and **2** is formed. For **2**, half an electron transfers from the left cage to the right cage, and **3** is formed. So **2** is simply the transition state. Its electron-transfer barrier was found to be 6.021 kcal mol^{-1}.

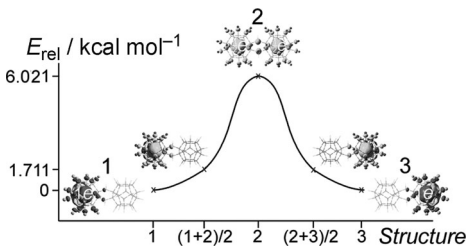

Figure 5. Potential curve of electron transfer at the LC-BLYP/6-311++G(d,p)+6s6p4d level, which shows that the electron prefers integrity to division.

As mentioned above, for isomers **1** and **3**, the excess electron is confined in the left and right $C_{20}F_{18}$ cage, respectively, while the excess electron is equally confined in both cages for **2**. The excess electron populations inside the left and right cages for the three isomers are 1:0 for **1**, 0.5:0.5 for **2**, and 0:1 for **3**. The (**1**+**2**)/2 (or (**2**+**3**)/2) in Figure 5 represents the structure between **1** and **2** (or **2** and **3**), which comes from averaging molecular coordinates of structures **1** and **2** (or **2** and **3**). Ratios of 0.75:0.25 and 0.25:0.75 are expected for the average electron populations in the intermediate structures (**1**+**2**)/2 and (**2**+**3**)/2, respectively. However, the SOMO in Figure 5 shows that the excess electron populations seem to be about 1:0 for (**1**+**2**)/2 and about 0:1 for (**2**+**3**)/2. This interesting results indicate that the average structure does not always correspond to average population, and the excess electron prefers integrity to division (charge transfer is a quantum quantity). This nature of the electron generally results in integral valences.

A comparison between the electron-transfer barrier and the work done by the electric field is interesting for the conversion **1**→**3**. The electric field (*F*) work *W* is [Eq. (3)]:

$$W = q_e\ F\ L_0 \qquad (3)$$

For the **1**→**3** electron transfer, $q_e = -1$, $F = -0.0001$ a.u., and $L_0 = 6.787$ Å (see Table 1), so *W* is 8.04 kcal mol^{-1}, which is close to the electron-transfer barrier of 6.021 kcal mol^{-1} but only 2 kcal mol^{-1} higher than it. This difference of 2 kcal mol^{-1} may mainly come from the different geometries used in calculations. The barrier of 6.021 kcal mol^{-1} comes from the optimized geometric structures of **1**, **2**, and **3**, matching the excess electron populations, while, the larger *W* comes from the frozen geometry of **1**, which has no energy saving due to geometric change in the electron-transfer process.

3. Conclusions

Owing to different locations of the excess electron inside cage(s), a new class of the intercage electron transfer isomers is found for $e^-@C_{20}F_{18}(NH)_2C_{20}F_{18}$. The three intercage electron transfer structures with two redox sites can be regarded as new nonmetal mixed-valent (0, −1) anions. Their synthesis is expected for two reasons. Firstly, many linked fullerenes have been reported experimentally, for example, σ-chain[39a] and π-chain.[39b] Secondly, some fluorinated fullerenes have been synthesized, in particular the $C_{20}F_{20}$ cage.[19]

The three radical intercage electron-transfer isomers have high reducibility close to that of the Cs atom and strong oxidizability similar to that of the O atom. They have different dipole moments μ_y of 13.4 (**1**), 0.0 (**2**), and −13.4 D (**3**), although **1** and **3** have the same E_{rel}, VDE, and VEA.

The interconversions among these isomers involve transfer of one or one-half excess electron from one cage to another. Two isomerism pathways are found: 1) Manipulation by external electric field to perform intercage electron transfer and 2) Excitation of the intercage electron-transfer transition from the ground to the first excited state of **1** (or **3**), whereby the electron simultaneously hops from inside the left cage to inside the right one, and a subsequent radiationless transition with retention of the electron inside the right cage can convert the first excited state of **1** to the ground state of **3** (or **1**), which achieves isomerism between **1** and **3**. Of course, the isomerism may accompany a change in physical properties, for instance, dipole moment. This suggests a control paradigm for the location and transportation of excess electron.

Interestingly, intercage electron-transfer isomers **1** and **3** have degenerate energy levels. The conversion between **1** and **3** is a microscopic electron-transfer process without proton transfer; its transition state just may be **2**, and its electron transfer barrier was also found to be 6.021 kcal mol^{-1}. The potential curve of the electron transfer in Figure 5 shows that electron prefers integrity to division. This is the reason that in general valences are integers.

This paper may be beneficial for many fields, such as isomerization, redox, microscopic electron transfer, radical and excess electron, and endohedral compounds. It may be useful for designing molecular photoelectron materials and electron-transfer devices.

Acknowledgements

This work was supported by the National Natural Science Foundation of China (No. 21173098, 21173095, and 21043003) the Foundation of State Key Laboratory of Theoretical and Computational Chemistry (China), and the Science and Technology Project of Jiangxi Provincial Department of Science & Technology (20114BAB213007).

Keywords: cage compounds · density functional calculations · electron transfer · isomerization · mixed-valent compounds

[1] S. Esteban, *J. Chem. Educ.* **2008**, *85*, 1201 – 1203.
[2] T. Bally, *Nat. Chem.* **2010**, *2*, 165 – 166.
[3] W. Kaim, A. Klein, M. Glockle, *Acc. Chem. Res.* **2000**, *33*, 755 – 763.
[4] *Mixed Valence Systems: Applications in Chemistry, Physics and Biology, Vol. 343* (Ed.: K. Prassides), NATO ASI Series C, Kluwer, Dordrecht, Holland, **1990**, pp. 91 – 106.
[5] H. I. Rayyat, W.-Z. Wang, G.-H. Lee, C.-Y. Yeh, S.-A. Hua, Y. Song, M.-M. Rohmer, M. Bénard, S.-M. Peng, *Angew. Chem.* **2011**, *123*, 2093 – 2096; *Angew. Chem. Int. Ed.* **2011**, *50*, 2045 – 2048.
[6] M. B. Robin, P. Day, *Adv. Inorg. Chem. Radiochem.* **1968**, *10*, 247 – 422.
[7] C. Creutz, H. Taube, *J. Am. Chem. Soc.* **1969**, *91*, 3988 – 3989.
[8] K. D. Demadis, C. M. Hartshorn, T. J. Meyer, *Chem. Rev.* **2001**, *101*, 2655 – 2686.
[9] C. Lambert, G. Nöll, *J. Am. Chem. Soc.* **1999**, *121*, 8434 – 8442.
[10] S. F. Nelsen, *Chem. Eur. J.* **2000**, *6*, 581 – 588.
[11] C. Desfrançois, S. Carles, J. P. Schermann, *Chem. Rev.* **2000**, *100*, 3943 – 3962.
[12] C. C. Page, C. C. Moster, X. Chen, L. Dutton, *Nature* **1999**, *402*, 47 – 52.
[13] H. M. Lee, S. Lee, K. S. Kim, *J. Chem. Phys.* **2003**, *119*, 187 – 194.
[14] Y. Li, Z.-R. Li, D. Wu, R.-Y. Li, X. Y. Hao, C.-C. Sun, *J. Phys. Chem. B* **2004**, *108*, 3145 – 3148.
[15] S. Matsuishi, Y. Toda, M. Miyakawa, K. Hayashi, T. Kamiya, M. Hirano, I. Tanaka, H. Hosono, *Science* **2003**, *301*, 626 – 629.
[16] Y.-F. Wang, Z.-R. Li, D. Wu, C.-C. Sun, F.-L. Gu, *J. Comput. Chem.* **2010**, *31*, 195 – 203.
[17] C.-Y. Zhang, H.-S. Wu, H. Jiao, *J. Mol. Model.* **2007**, *13*, 499 – 503.
[18] Y.-F. Wang, Z.-R. Li, D. Wu, Y. Li, C.-C. Sun, F.-L. Gu, *J. Phys. Chem. A* **2010**, *114*, 11782 – 11787.
[19] F. Wahl, A. Weiler, P. Landenberger, E. Sackers, T. Voss, A. Haas, M. Lieb, D. Hunkler, J. Wörth, L. Knothe, H. Prinzbach, *Chem. Eur. J.* **2006**, *12*, 6255 – 6267.
[20] J. Simons, *J. Phys. Chem. A* **2008**, *112*, 6401 – 6511 and references therein.
[21] I. A. Shkrob, *J. Phys. Chem. A* **2007**, *111*, 5223 – 5231.
[22] J. C. Rienstra-Kiracofe, G. S. Tschumper, H. F. Schaefer III, N. Sreela, G. B. Ellison, *Chem. Rev.* **2002**, *102*, 231 – 282.
[23] L. Zhang, S. Yan, R. I. Cukier, Y. Bu, *J. Phys. Chem. B* **2008**, *112*, 3767 – 3772.
[24] P. Skurski, M. Gutowski, J. Simons, *Int. J. Quantum Chem.* **2000**, *80*, 1024 – 1038.
[25] Gaussian 09 (Revision A.02), M. J. Frisch, G. W. Trucks, H. B. Schlegel, G. E. Scuseria, M. A. Robb, J. R. Cheeseman, G. Scalmani, V. Barone, B. Mennucci, G. A. Petersson, H. Nakatsuji, M. Caricato, X. Li, H. P. Hratchian, A. F. Izmaylov, J. Bloino, G. Zheng, J. L. Sonnenberg, M. Hada, M. Ehara, K. Toyota, R. Fukuda, J. Hasegawa, M. Ishida, T. Nakajima, Y. Honda, O. Kitao, H. Nakai, T. Vreven, J. A. Montgomery, Jr., J. E. Peralta, F. Ogliaro, M. Bearpark, J. J. Heyd, E. Brothers, K. N. Kudin, V. N. Staroverov, R. Kobayashi, J. Normand, K. Raghavachari, A. Rendell, J. C. Burant, S. S. Iyengar, J. Tomasi, M. Cossi, N. Rega, J. M. Millam, M. Klene, J. E. Knox, J. B. Cross, V. Bakken, C. Adamo, J. Jaramillo, R. Gomperts, R. E. Stratmann, O. Yazyev, A. J. Austin, R. Cammi, C. Pomelli, J. W. Ochterski, R. L. Martin, K. Morokuma, V. G. Zakrzewski, G. A. Voth, P. Salvador, J. J. Dannenberg, S. Dapprich, A. D. Daniels, O. Farkas, J. B. Foresman, J. V. Ortiz, J. Cioslowski, D. J. Fox, Gaussian, Inc., Wallingford CT, 2009 Gaussian, Inc., Wallingford, CT, **2009**.
[26] M. Lundberg, P. E. M. Siegbahn, *J. Chem. Phys.* **2005**, *122*, 224103.
[27] P. Mori-Sánchez, A. J. Cohen, W. T. Yang, *J. Chem. Phys.* **2006**, *125*, 201102.
[28] X. Ren, A. Tkatchenko, P. Rinke, M. Scheffler, *Phys. Rev. Lett.* **2011**, *106*, 153003.
[29] M.-C. Kim, E. Sim, K. Burke, *J. Chem. Phys.* **2011**, *134*, 171103.
[30] a) M. Boero, M. Parrinello, K. Terakura, T. Ikeshoji, C. C. Liew, *Phys. Rev. Lett.* **2003**, *90*, 226403; b) G. W. Morley, B. J. Herbert, S. M. Lee, K. Porfyrakis, T. J. S. Dennis, D. Nguyen-Manh, R. Scipioni, J. Van Tol, A. Phorsfield, A. Ardavan, D. G. Pettifor, J. C. Green, G. A. D. Briggs, *Nanotechnology* **2005**, *16*, 2469 – 2473.
[31] a) J. V. Coe, S. M. Williams, K. H. Bowen, *Int. Rev. Phys. Chem.* **2008**, *27*, 27 – 51; b) D. R. Lide, *CRC Handbook of Chemistry and Physics*, CRC Press, Boca Raton, **2000**.
[32] Z.-J. Zhou, X.-P. Li, Z.-B. Liu, Z.-R. Li, X.-R. Huang, C.-C. Sun, *J. Phys. Chem. A* **2011**, *115*, 1418 – 1422.
[33] a) E. Cieluch, K. Pietryga, M. Sarewicz, A. Osyczka, *Biophysica. Acta.* **2010**, *1797*, 296 – 303; b) A. C. Benniston, A. Harriman, P. Li, *J. Am. Chem. Soc.* **2010**, *132*, 26 – 27.
[34] J. S. Park, E. Karnas, K. Ohkubo, P. Chen, K. M. Kadish, S. Fukuzumi, C. W. Bielawski, T. W. Hudnall, V. M. Lynch, J. L. Sessler, *Science* **2010**, *329*, 1324 – 1327.
[35] X.-Y. Li, F.-C. He, *J. Comput. Chem.* **1999**, *20*, 597 – 603.
[36] J. Stubbe, D. G. Nocera, C. S. Yee, M. C. Y. Chang, *Chem. Rev.* **2003**, *103*, 2167 – 2201.
[37] X. Chen, Y. Bu, *J. Am. Chem. Soc.* **2007**, *129*, 9713 – 9720.
[38] G. N. Sastry, S. Shaik, *J. Phys. Chem.* **1996**, *100*, 12241 – 12252.
[39] a) J. Zhang, K. Porfyrakis, J. J. L. Morton, M. R. Sambrook, J. Harmer, L. Xiao, A. Ardavan, G. A. D. Briggs, *J. Phys. Chem. C* **2008**, *112*, 2802 – 2804; b) T. J. Hingston, M. R. Sambrook, N. H. Reesb, K. Porfyrakis, G. A. D. Briggs, *Tetrahedron Lett.* **2006**, *47*, 8595 – 8597.

Received: October 8, 2011
Published online on February 8, 2012

